New Polylactide/Layered Silicate Nanocomposites: Role of Organoclays

Pralay Maiti,[†,||] Kazunobu Yamada,[‡] Masami Okamoto,*[,†] Kazue Ueda,[‡] and Kazuaki Okamoto[§]

Advanced Polymeric Materials Engineering, Graduate School of Engineering, Toyota Technological Institute, Hisakata 2-12-1, Tempaku, Nagoya 468 8511, Japan, Unitika Ltd., Kozakura 23, Uji, Kyoto 611-0021, Japan, and Nagoya Municipal Research Institute, Rokuban 3-4-41, Atsuta, Nagoya 456-0058, Japan

Received April 16, 2002. Revised Manuscript Received September 13, 2002

In the preparation of polymer/clay nanocomposites, organoclay plays an important role in lipophilizing and dispersing the clay into less polar polymer matrixes. Organic modifiers of various chain lengths were examined in different types of clays, smectite, montmorillonite (MMT), and mica, to prepare their corresponding organoclays. The layered structure and gallery spacing of organoclays and polylactide (PLA) nanocomposites shows that, with a modifier of the same chain length, the gallery spacing of the organoclay was largest for mica and smallest for smectite because of the higher ion-exchange capacity of mica and physical jamming of the modifier due to a restricted conformation at the core part of the clay of larger size. The increment of the modulus in a smectite nanocomposite, compared to that of PLA, is higher than MMT or mica nanocomposite due to better dispersion in a smectite system for the same clay loading. Being a well-dispersed system, smectite nanocomposites have better gas barrier properties than the MMT or mica systems, which are larger in size but stacked in nature in their nanocomposites. A new idea for obtaining porous ceramic material from layered silicate/polymer nanocomposites by burning is unveiled using various clays and the mechanism of their formation is elucidated.

Introduction

An interesting aspect of poly(lactic acid) (PLA) is its availability from a monomer/cyclic dimer (lactide) produced by fermentation of agricultural crops such as corn, potato, and waste products. Because of this "green" feature combined with its benign degradation behavior, PLA is considered as a potential packaging material in many fields. Biomedical uses of PLA have been widespread, which include bioabsorbable surgical sutures and implants,[1] controlled drug delivery,[2] and tissue culture.[3] However, the strength and some other properties such as thermal stability, gas barrier, solvent resistance, and flame retardance of the pure polymer are often not enough for end use. Confinement of polymer in a two-dimensional silicate gallery, so-called polymer nanocomposite,[4−11] is one of the effective ways to improve material performance. Ogata et al.[12] first prepared blends of PLA and organically modified clay by the solution casting method but they found only tactoids, which consist of several stacked silicate layers. As a result, the modulus of the blend is slightly higher than that of PLA. In our previous article,[13] we successfully prepared the ordered and well-dispersed nanocomposites of PLA using octadecylammonium-modified montmorillonite (MMT). Uses of phosphonium salt as a modifier has another advantage, higher thermal stability than ammonium salt. Recently, Zhu et al.[14] reported one phosphonium modifier to improve the firing properties of polystyrene/clay nanocomposites. An organic modifier has the important role of making a

* To whom correspondence should be addressed. E-mail: okamoto@toyota-ti.ac.jp.
† Toyota Technological Institute.
‡ Unitika Ltd.
§ Nagoya Municipal Research Institute.
|| Present address: Material Science and Engineering, Cornell University, 214 Bard Hall, Ithaca, NY 14853.

(1) Taylor, M. S.; Daniels, A. U.; Andriano, K. P.; Heller, J. *J. Appl. Biomater.* **1994**, *5*, 151.
(2) Park, T. G.; Cohen, S.; Langer, R. *Macromolecules* **1992**, *25*, 116; US Patent, 5330768, 1994.
(3) Kohn, J. *MRS Bull.* **1996**, *21*, 18. Mikos, A. G.; Lyman, M. D.; Freed, L. E.; Langer, R. *Biomaterials* **1994**, *15*, 55.
(4) Giannelis, E. P. *Adv. Mater.* **1996**, *8*, 29.
(5) Garces, J. M.; Moll, D. J.; Bicerano, J.; Fibiger, R.; McLeod, D. G. *Adv. Mater.* **2000**, *12*, 1835.
(6) LeBaron, P. C.; Wang, Z.; Pinnavaia, T. J. *Appl. Clay Sci.* **1999**, *15*, 11.
(7) Vaia, R. A.; Ishii, H.; Giannelis, E. P. *Chem. Mater.* **1993**, *5*, 1694. Vaia, R. A.; Teukolsky, R. K.; Giannelis, E. P. *Chem. Mater.* **1994**, *6*, 1017. Vaia, R. A.; Vasudevan, S.; Krawice, W.; Scanlon, L. G.; Giannelis, E. P. *Adv. Mater.* **1995**, *7*, 154.
(8) Usuki, A.; Kojima, Y.; Kawasumi, M.; Okada, A.; Fukushima, Y.; Kurauchi, T.; Kamigaiti, O. *J. Mater. Res.* **1993**, *8*, 1179. Kawasumi, M.; Hasegawa, N.; Kato, M.; Usuki, A.; Okada, A. *Macromolecules* **1997**, *30*, 6333. Hasegawa, N.; Kawasumi, M.; Kato, M.; Usuki, A.; Okada, A. *J. Appl. Polym. Sci.* **1998**, *67*, 87.
(9) Lan, T.; Kaviratna, P. D.; Pinnavaia, T. J. *Chem. Mater.* **1994**, *6*, 573. Shi, H.; Lan, T.; Pinnavaia, T. J. *Chem. Mater.* **1996**, *8*, 1584.
(10) Alexandre, M.; Dubois, P. *Mater. Sci. Eng., R.* **2000**, *28*, 1.
(11) Maiti, P.; Nam, P. H.; Okamoto, M.; Hasegawa, N.; Usuki, A. *Macromolecules* **2002**, *35*, 2042. Maiti, P.; Nam, P. H.; Okamoto, M.; Kotaka, T.; Hasegawa, N.; Usuki, A. *Polym. Eng. Sci.* **2002**, *42*, 1864.
(12) Ogata, N.; Jimenez, G.; Kawai, H.; Ogihara, T. *J. Polym. Sci., Part B: Polym. Phys.* **1997**, *35*, 389.
(13) Sinha Ray, S.; Maiti, P.; Okamoto, M.; Yamada, K.; Ueda, K. *Macromolecules* **2002**, *35*, 3104.
(14) Zhu, J.; Morgan, A. B.; Lamelas, F. J.; Wilkie, C. A. *Chem. Mater.* **2001**, *13*, 3774.

10.1021/cm020391b CCC: $22.00 © 2002 American Chemical Society
Published on Web 10/31/2002

Table 1. Name, Chemical Formula, and Designation of the Organic Modifiers Used

name and formula	designated as
$[(C_4H_9)_3P(C_8H_{17})]^+ Br^-$ *n*-octyl tri-*n*-butyl phosphonium bromide	C_8
$[(C_4H_9)_3P(C_{12}H_{25})]^+ Br^-$ *n*-dodecyl tri-*n*-butyl phosphonium bromide	C_{12}
$[(C_4H_9)_3P(C_{16}H_{33})]^+ Br^-$ *n*-hexadecyl tri-*n*-butyl phosphonium bromide	C_{16}
$[(C_6H_5)_3P(CH_3)]^+ Br^-$ methyl triphenyl phosphonium bromide	C_{Ph}

nanocomposite either by suitably mixing with a matrix polymer and thus enhancing interaction with clay and polymer in the gallery or by dictating the gallery spacing by changing the chain length of the modifier, and hence favoring intercalation. Considering the clay particles as disk-shaped, the aspect ratio, defined as the ratio of diameter to thickness, of clay particles play an important role for the enhancement of properties. To the best of our knowledge, there is no systematic report on how the aspect ratio of clay affects the properties of nanocomposites. Another advantage of nanocomposites is their improved barrier properties in the presence of a few percent of high-aspect-ratio clay particles, retaining the flexibility and optical clarity of pure polymer.[15,16] Porous materials/ceramic foams can be produced by various methods[17] and their unique behavior such as high thermal stability, low thermal conductivity, low density, high permeability, and chemical resistance is reported in earlier works.[18−20] A polymer layered silicate nanocomposite might be a good source for preparing porous ceramic material just by burning at high temperature. There is no report of a comparative study of dispersion and aspect ratio of clay affecting the final properties of nanocomposites.

In this paper, first we present the effect of a phosphonium modifier of different chain lengths on the properties of organoclay and how the different clays behave differently having the same organic modifier. Second, the effects of dispersion, intercalation, and aspect ratio of clay on properties such as mechanical strength, gas barrier, and porous ceramics of nanocomposites were examined.

Experimental Section

Materials and Preparation. Polylactide (PLA) ($M_w = 1.87 \times 10^5$, $M_w/M_n = 1.76$ and *D* content = 1.1−1.7%) used in this study was supplied by Unitika Co. Ltd., Japan, and dried under vacuum at 80 °C before the preparation of the nanocomposite. Four different types of organic modifier, having different chain lengths, were used in this work and their names, chemical formulas, and designations (as written in the text) are presented in Table 1. Henceforth, we will term the methyl triphenyl phosphonium bromide, *n*-octyl tri-*n*-butyl phosphonium bromide, *n*-dodecyl tri-*n*-butyl phosphonium bromide, and *n*-hexadecyl tri-*n*-butyl phosphonium bromide as C_{Ph}, C_8, C_{12}, and C_{16}, respectively. Three different natural/synthetic clays were used, namely, montmorillonite (MMT) (natural clay supplied by Shiraishi Ltd., Japan), smectite (as called by the supplier, COOP Chemical Co. Ltd., Japan), and mica (synthetic clays from COOP Chemical). Organoclays of smectite with all four of the above-mentioned modifiers had been prepared and organoclays of MMT and mica were prepared with C_{16} modifier. Chloroform (Wako Chemical Industries Ltd.) was used as a solvent for PLA and organic modifiers.

Table 2. Characteristics of Nanocomposites (Designation, Type of Clay, Organic Modifier, and Clay Content)

	type of clay	organic modifier	wt % of clay in nanocomposites (inorganic part)
PLACN1	smectite	C_{16}	1.2
PLACN2	smectite	C_{16}	3
PLACN3	smectite	C_{16}	4
PLACN4	smectite	C_{16}	5
PLACN5	MMT	C_{16}	3
PLACN6	MMT	C_{16}	3.8
PLACN7	MMT	C_{16}	5
PLACN8	mica	C_{16}	2.8
PLACN9	mica	C_{16}	3.8
PLACN10	mica	C_{16}	5
PLACN11	smectite	C_{12}	3.2
PLACN12	smectite	C_8	1.7
PLACN13	smectite	C_{Ph}	3.5

The nanocomposites of PLA (PLACNs) were prepared through the melt extrusion method with PLA and different organoclays using a twin-screw extruder (S-1 KRC, Kurimoto Ltd.) operated at 190 °C after they were shaken in a bag. The extruded and pelletized strands were dried under vacuum at 80.0 °C to remove residual water. The clay content in the nanocomposites was varied by mixing different amounts of organoclay with PLA. The nature of the clay, modifier, and clay contents are summarized in Table 2. As usual, the molecular weight of PLA decreased after the PLA was extruded with clay at 190.0 °C but degradation is not severe (e.g., PLA ($M_w = 1.87 \times 10^5$) and PLACN2 ($M_w = 1.5 \times 10^5$); however, it has to be noted that degradation can be stopped by using other types of clay as in our previous work.[13] The inorganic part of the nanocomposite was measured by burning it at 950 °C in a furnace. PLACNs were characterized by using wide-angle X-ray diffraction (WAXD), transmission electron microscopy (TEM) observation, and a dynamic mechanical analyzer. Blends of PLA and organic modifiers (60:40) were prepared by the solution casting method and their miscibility was checked by measuring the T_g using a differential scanning calorimeter (DSC).

Preparation of Porous Ceramic. A thick sheet of PLACN was melted in a furnace in the presence of air from room temperature to 350 °C, as thermogravimetric (TG) data show degradation of PLA starts at 300 °C, at the heating rate of 10°/min, was maintained at that temperature for 1 h, and then was heated again to 950 °C until its complete burning. White or slight gray colored (depending on the clay used) flake-like materials appeared on the crucible and the morphology of the fracture surface of the ceramic was examined by using a scanning electron microscope (SEM).

DSC. The samples were characterized by using a temperature-modulated differential scanning calorimeter, operated in the conventional DSC mode (TMDSC, TA2920, TA Instruments), at the heating rate of 5 °C/min, to determine the glass transition temperature (T_g), crystallization temperature (T_c), and melting temperature (T_m) of PLA and PLACNs. The samples were heated to 200.0 °C, maintained at that temperature for 5 min to remove the thermal history, and quenched to −20 °C at the heating rate of 40 °C/min. The second run was taken for the determination of T_g, T_c, and T_m. The DSC was calibrated with indium before use.

WAXD. X-ray diffraction experiments were performed using a MXlabo diffractometer (MAC Science Co.) with Cu Kα radiation and a graphite monochromator (wavelength, $\lambda = 0.154$ nm). The generator was operated at 40 kV and 20 mA.

(15) Yano, K.; Usuki, A.; Okada, A. *J. Polym. Sci., Part A*: *Polym. Chem*. **1997**, *35*, 2289.
(16) Xu, R. J.; Manian, E.; Snyder, A. J.; Runt, J. *Macromolecules* **2001**, *34*, 337.
(17) Davis, G. J.; Zhen, S. *J. Mater. Sci*. **1983**, *18*, 1899.
(18) Rice, R. W. *Porosity of Ceramics*; Marcel Dekker: New York, 1998.
(19) Colombo, P.; Modesti, M. *J. Am. Ceram. Soc*. **1999**, *19*, 2059.
(20) Gibsob, L. J.; Ashby, M. F. *Cellular Solids*; Pergamon Press: New York, 1998.

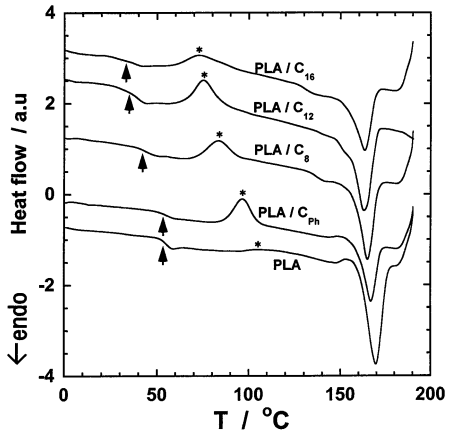

Figure 1. DSC thermograms of blends of PLA with different phosphonium salts indicated in the figure. The upper head arrows show the T_g of the blends and the asterisks show the cold crystallization temperatures.

The melt-quenched samples were placed inside a copper sample holder at room temperature and were scanned at diffraction angle 2θ from 2° to 10° at the scanning rate of 0.5°/min.

TEM. The dispersibility of the clay particles in the matrix was checked by using TEM (H-7100 Hitachi Co.) operated at an accelerating voltage of 100 kV without staining. A thin layer, around 80-nm thick, from the crystallized sample was sectioned at −80.0 °C using a Reichert ultra-microtome equipped with a diamond knife.

Dynamic Mechanical Characterization. Dynamic mechanical measurements were performed on the samples 35 × 12 × 0.5 mm^3 in size, annealed at 120 °C for 1 h, using dynamic temperature ramp tests, on a Rheometrics Dynamic Analyzer (RDAII) in tension-torsion mode in the temperature range between −20.0 and 150.0 °C at the heating rate of 2 °C/min, keeping the strain amplitude of 0.05%. The angular frequency, ω, for the experiments was 6.28 rad/s.

Measurement of Gas Permeability. Oxygen gas transmission rates of PLA and PLACNs were measured at 20 °C and 90% relative humidity by the ASTM D 1434 constant pressure method (Yanaco GTR-30XAU). Specimens were prepared by compression molding (≈200 μm) and melt-quenched amorphous samples were used for this study.

SEM. The morphology of the fracture surface of ceramic material was examined with a JSM-5900LV (JEOL) instrument operated at 10 kV. All the samples were gold-coated by means of a JFC-1600 (JEOL) sputtering apparatus before observation.

Results and Discussion

Miscibility. The first criterion for choosing the organic modifier is that it should be miscible with the matrix polymer. Figure 1 shows the DSC thermograms of blends of PLA with different organic modifiers (60:40) listed in Table 1. The arrows indicate the position of the glass transition temperature (T_g) for each blend and the asterisks show the cold crystallization temperatures (T_c) of each system. It is clear from the figure that C_{Ph} salt is immiscible with PLA and has the same T_g as PLA and depression of T_g occurs with an increase of chain length of the modifier from C_8 to C_{16}; that is, the miscibility increases with the chain lengths of the modifiers. T_c also decreases with chain length, indicating pronounced nucleating behavior of a higher chain length modifier. Accordingly, the melting temperature (T_m) of PLA decreases gradually with increasing chain length. All these phenomena suggest that C_{16} salt has one of the highest miscibilities with PLA and, hence, is the best choice as an organic modifier for preparing organoclay.

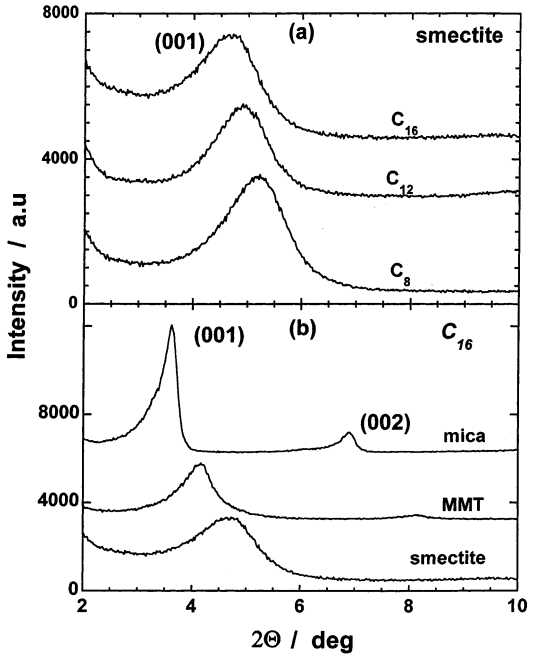

Figure 2. WAXD patterns of organically modified clay: (a) smectite clay modified with C_8, C_{12}, and C_{16} phosphonium salt; (b) smectite, MMT, and mica clay modified with C_{16} phosphonium salt.

Organoclays: Chain Length of Organic Modifier and Aspect Ratio of Clay. Figure 2a shows WAXD patterns of smectite organoclays with C_8, C_{12}, and C_{16} as the modifiers. The peak angles are shifting toward a lower 2θ region with increasing chain length, indicating higher gallery spacing for a modifier having a longer chain. The gallery spacing, $d_{(001)}$, is 1.69, 1.78, and 1.87 nm for C_8, C_{12}, and C_{16} smectite organoclays, respectively. Usuki et al.[21] reported basal spacing of 1.34 nm for C_8 to 2.82 nm for C_{18} using MMT and amino acid as the organic modifier, but we did not find such drastic change, especially for the long-chain modifier in smectite organoclay. Most likely, the reason lies in the aspect ratio of clay, which will be clear in our subsequent discussion. Anyway, the WAXD patterns of smectite, MMT, and mica with the same C_{16} modifier are presented in Figure 2b. It is obvious that $d_{(001)}$ is in the order smectite (1.87 nm) < MMT (2.13 nm) < mica (2.44 nm). The characteristics of clays/organoclays are presented in Table 3.

The d spacing ($d_{(001)}$) increases with modifier chain length and for a fixed modifier it increases with increasing lateral dimension of the clay particle. Here, it has to be mentioned that the cation-exchange capacity (CEC) of natural/synthetic clay is in the order smectite < MMT < mica (Table 3). From the supplier's data it is believed that Na^+ ion present in the clay is fully replaced by phosphonium (P^+) ion during the ion-exchange process. So, from the CEC data, the amount of P^+ (modifier) present in the silicate galleries is in the order smectite < MMT < mica. There is another factor, which lies in the size of the clay. In mica, being larger in size and having a greater number of modifiers,

(21) Usuki, A.; Kawasumi, M.; Kojima, Y.; Okada, A.; Kurauchi, T.; Kamigaito, O. *J. Mater. Res.* **1993**, *8*, 1174.

Table 3. Characteristics of the Clays Used (Natural, Organically Modified, and in Nanocomposites)

	smectite	MMT	mica
size[a] (nm)	50−60	100−130	200−300
CEC (mequiv/100 g)	87	113	120
$d_{(001)}$[b] (clay) Na^+ (nm)	1.2	1.2	1.25
$d_{(001)}$[b] (organoclay with C_{16} salt) (nm)	1.87	2.13	2.44
$d_{(001)}$[b] in nanocomposites with C_{16} clay (≈3 wt %) (nm)	2.27	2.55	2.69
crystallite size[c] of organoclay with C_{16} salt (nm)	7	12	20
crystallite size[c] in nanocomposites (≈3 wt %) clay (nm)	3.5	10	22

[a] Size of organically modified clay as observed in TEM micrograph of nanocomposite. [b] Calculated from wide-angle X-ray diffraction data. [c] Calculated from Scherrer equation $D_{hkl} = (k\lambda)/(\beta \cos \theta)$, where k is a constant, λ is the wavelength, β is the half-width, and θ is the peak angle.

Scheme 1

Schematic representation of organoclays with C_{16} ion

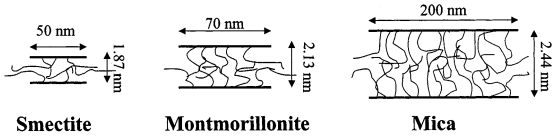

organic modifiers present at the core have restricted conformation due to physical jamming. This physical jamming is smaller in the case of smectite clay due to a lower CEC and smaller size. Therefore, the situation for organoclays, based on TEM and WAXD data, are schematically represented in Scheme 1. Another important factor is that the coherency of the organoclay increases with increasing lateral size of the clay (Figure 2b), while for one clay system, smectite with a different modifier, the coherency is almost the same (Figure 2a). From the WAXD patterns the crystallite sizes of different organoclays are calculated by using the Scherrer equation and are reported in Table 3. It is evident from the table that stacking of organoclay increases with the size and CEC of clay and it is maximum in the case of mica. It is believed that, out of two factors, the density of organo-modification (CEC) plays the more important role, determining the *d*-spacing/stacking of silicate layers.

Microstructure of Nanocomposites. Figure 3 shows the nature of the modifier and chain length dependency on intercalation of PLA using smectite organoclays. The dotted lines are the peak positions of the corresponding organoclays. No intercalation of PLA occurs in the case of C_{Ph}- and C_8-clay nanocomposites. C_{Ph} salt is immiscible with PLA, so the question of intercalation does not appear.[22] But the space between silicate galleries in C_8 organoclay is not sufficient (≈1.69 nm) for intercalation, even though interaction exists between PLA and C_8 salt. Slight shifting of peak occurs toward a lower angle in the case of PLACN11 and C_{12} organoclay is the borderline case where intercalation begins. The literature-reported value[21] for making intercalated species is also more than that for C_{11} for an amino acid modifier in MMT. With a further increase of modifier chain length to C_{16} organoclay, the peak shifts significantly to a lower angle in PLACN2, indicating well-dispersed nanocomposites.

(22) We measured the $d_{(001)}$ spacing using WAXD of oligo-poly(ϵ-caprolactone) (*o*-PCL, molecular weight = 500) suspension with different types of organoclay. The C_{Ph} system shows no intercalation up to 25 wt % of organoclay loading while the C_8 to C_{16} systems exhibit intercalation in every clay loading. Even though it is small in size, *o*-PCL cannot intercalate owing to its immiscibility with C_{Ph} salt but it is miscible with C_8 salt and higher homologues and thus can be intercalated easily.

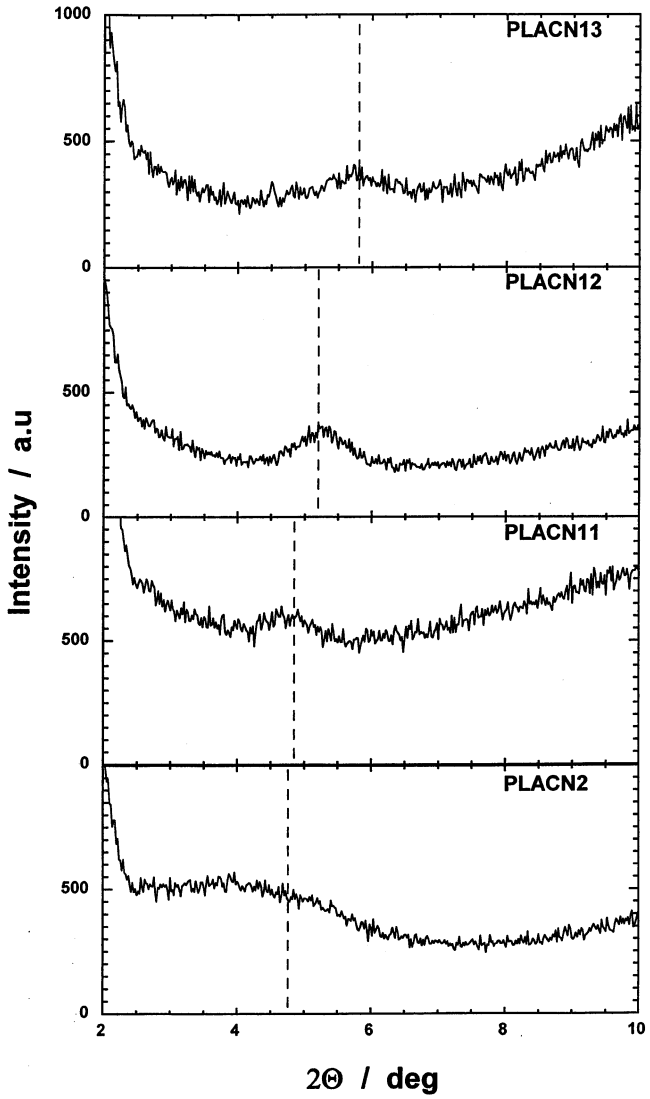

Figure 3. WAXD patterns of smectite-organoclay nanocomposites having different organic components (chain length dependency on intercalation). The broken lines represent the peak position of the corresponding organoclay.

The morphologies of PLACN12 and PLACN2 are shown in Figure 4. It is clear from the figures that stacked silicates layers are evident in PLACN12 (Figure 4a), while good dispersion appears in PLACN2 (Figure 4b). From the morphology, we can explain well the WAXD patterns of the nanocomposites. Due to a well-dispersed morphology in PLACN2, the peak becomes broad while for the nonintercalated stacked structure in PLACN12, the peak position is the same as that of the organoclay. Figure 5 shows the clay content dependency on intercalation of smectite-C_{16} nanocomposites.

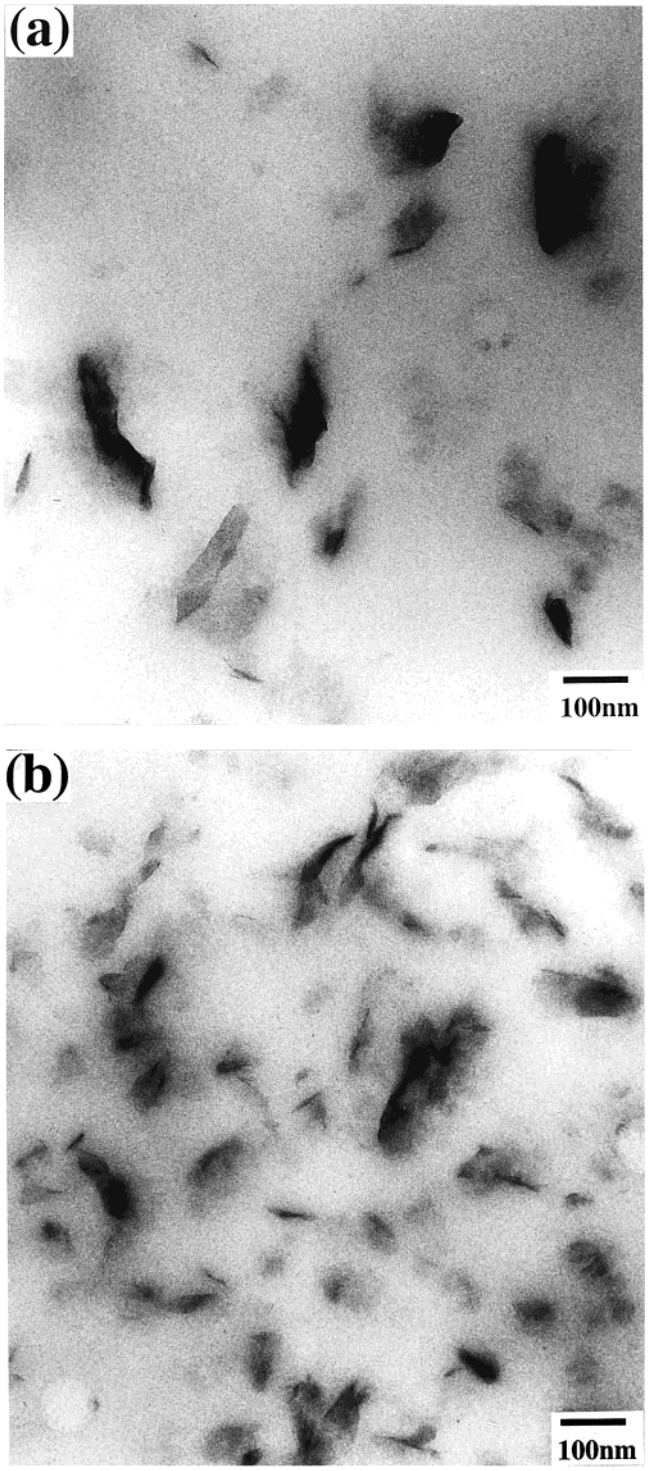

Figure 4. Bright field transmission electron micrographs of (a) PLACN12 (C_8, 1.7 wt %) and (b) PLACN2 (C_{16}, 3 wt %).

The peak intensity increases with increasing clay content, but in general, a less ordered structure appears in the case of smectite nanocomposites, especially at low clay content. On the other hand, nanocomposites of MMT and mica are intercalated and well-ordered. Figure 6 compares the WAXD patterns of nanocomposites with different clay dimensions having the same clay (C_{16}-modified) content (≈3 wt %). The verticle line on each curve represents the peak position of the organoclay. Coherency of the nanocomposites is in the order smectite < MMT < mica. The crystallite size, calculated from the Scherrer equation, and $d_{(001)}$ of the nanocomposites are reported in Table 3. The crystallite size of smectite nanocomposites (3.5 nm) becomes half compared to that of its corresponding organoclay (7 nm). Broad peak and small crystallite size suggest that smectite nanocomposites are well-dispersed and less ordered. For MMT nanocomposites, the peaks are sharp and crystallite sizes are slightly less than those of the corresponding organoclay, indicating a more ordered structure in MMT nanocomposites. The peaks of mica nanocomposites are very sharp, similar to those of its organoclay, and slightly larger crystallite sizes indicate that the number of stacked silicate layers is the same but some amount of PLA is intercalated between the galleries, giving rise to a larger crystallite size. On the basis of the diffraction pattern and crystallite size, stacking of silicate layers in the organoclays and in nanocomposites in three different organoclay systems are shown in Scheme 2.

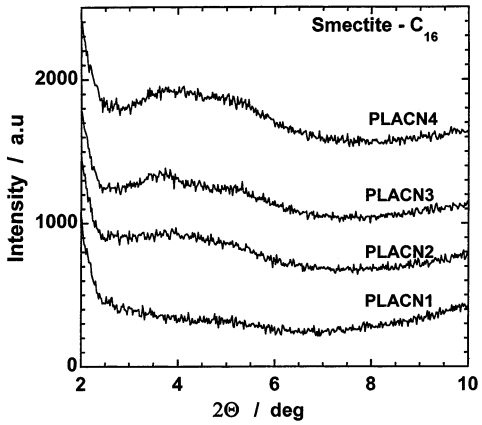

Figure 5. WAXD patterns of C_{16}-smectite clay nanocomposites: clay content dependency.

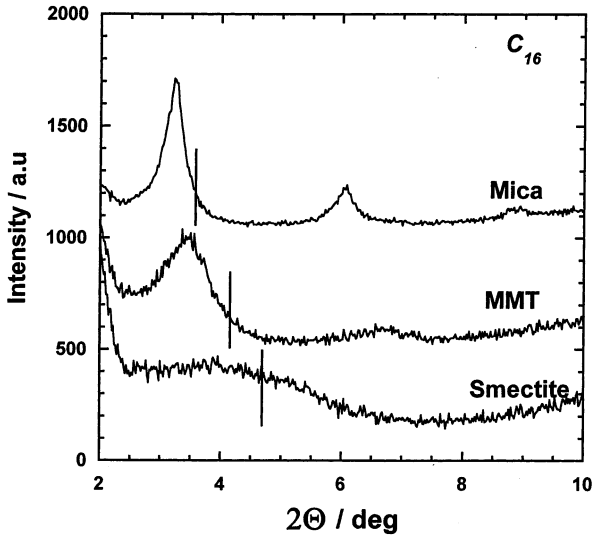

Figure 6. WAXD patterns of smectite, MMT, and mica nanocomposites with C_{16} organoclay and same clay content (3 wt %).

Now, it is necessary to discover the stacking behavior of silicate layers in organoclays/nanocomposites together with the intercalation mechanism. For a particular organic modifier, the nature of interaction between modifier and polymer matrix/silicate layer is the same, considering the same chemical nature of the clays. The only factor is the size of the clay, which determines the

Scheme 2

Stacking of silicate layers in organoclay and in nanocomposites

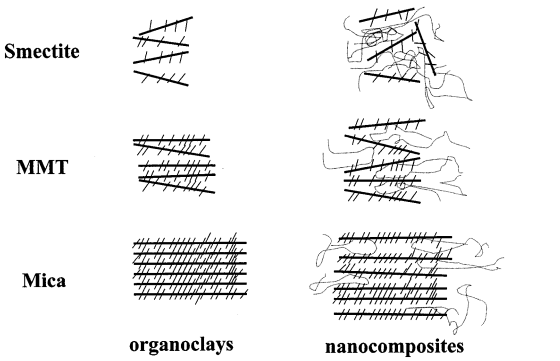

stacking of layers especially in organoclay. Smectite clay, being smaller in size (≈50 nm), is easy to distort by mechanical means and, therefore, has a broad peak and smaller crystallite size. But it is difficult to distort the stacking in mica because of its size (≈200−250 nm). Similar things happen for nanocomposites. Even though the extent of interaction is the same in all cases but in mica, due to its nicely stacked nature, polymer chains cannot penetrate up to the core of the silicate layers (Scheme 2), while in the case of smectite clay the polymer chain can easily penetrate, due to its smaller size, in an already less ordered stacking of organoclay, resulting in a well-dispersed, lesser ordered nanocomposite. This kinetic effect of the mobility of the polymer chains into the silicate galleries should have some time-dependent phenomena like polypropylene nanocomposites.[11] MMT always has the intermediate situation both for organoclays and for nanocomposites; as a result, moderately ordered and well-intercalated nanocomposites appear.

Mechanical Property: Organoclay Dependency. Figure 7a shows the storage modulus, G', of PLA and PLACN12 (C_8 nanocomposite, clay content 1.7 wt %). The G' of PLA and nanocomposites at 20 °C is measured and presented in Table 4. At the same condition, a 13.9% increment of modulus occurs in the case of PLACN12 compared to that in PLA. The G' of C_{16} nanocomposites have been shown in Figure 7b. PLACN1 (clay content 1.2 wt %) and PLACN3 (clay content 4 wt %) exhibit a 46.7 and 65.5% increment of G', respectively. From the WAXD and TEM observation, it is evident that C_8- and C_{16}-smectite clay nanocomposites are nonintercalated and intercalated (less ordered) types, respectively. Being the conventional type of composite, the C_8 system exhibits a smaller increment (13.9%) while the C_{16} system shows better mechanical property (46.7% increment for comparable clay content) due to its nanoscale dispersion in a polymer matrix.

The increment of G' in MMT and mica nanocomposite (PLACN6 and PLACN9), both having the same clay loading and same type of intercalated and well-ordered structure, is 24.8 and 41.2%, respectively, compared to that of PLA (Table 4). The higher increment in G' of mica nanocomposite is explained from its higher aspect ratio. But if we compare G' of the smectite and mica system (PLACN3 and PLACN9), having almost the same clay content, the smectite system exhibits better mechanical property (65.5% increment) than the mica system (41.2%). Here, in the smectite system, the dispersion is good and that plays a significant role in improving the property. The nature of stacked silicate layers in MMT and mica nanocomposites is confirmed from their respective TEM bright field images.

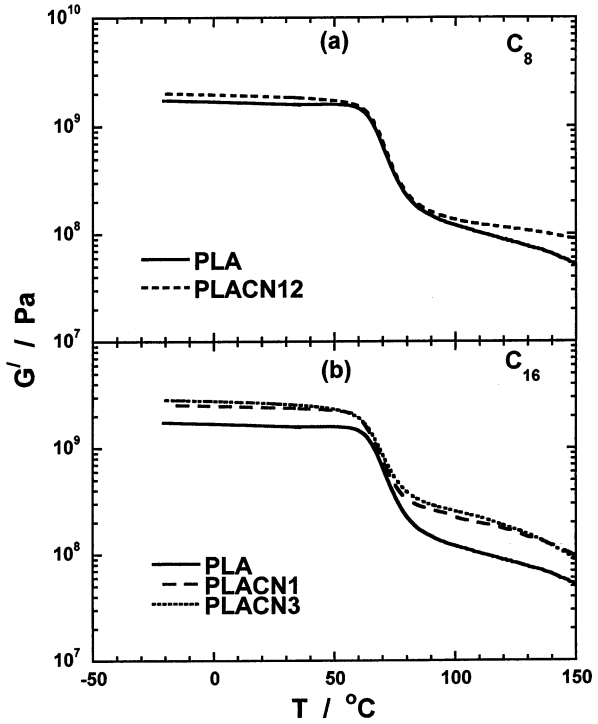

Figure 7. Storage modulus, G', of (a) PLA and PLACN12, nanocomposite having C_8-smectite organoclay and (b) PLA and nanocomposites with C_{16}-smectite organoclay and its clay content dependency.

Table 4. Storage Modulus, G', of PLA and Nanocomposites of Different Systems

	G' at 20 °C (GPa)	% increment compared to PLA at same temperature
PLA	1.65	
PLACN1	2.42	46.7
PLACN2	2.47	49.7
PLACN3	2.73	65.5
PLACN6	2.06	24.8
PLACN9	2.33	41.2
PLACN12	1.88	13.9

Table 5. Oxygen Gas Permeability of PLA and Nanocomposites

sample	O_2 transmittance × 10^{-3} (mL μm m^{-2} day^{-1} MPa^{-1}
PLA	200
PLACN1	150
PLACN3	120
PLACN6	121
PLACN9	144

Finally, the combined effect of aspect ratio and dispersion of clay particles ultimately control the mechanical property of the nanocomposite but dispersion plays the major role.

Oxygen Gas Permeability: Clay Dependency. Table 5 represents the oxygen gas permeability per unit of micrometer thickness of PLA and nanocomposite sample in the amorphous state. PLACN1 (smectite clay content 1.2 wt %) has the permeability 150 × 10^3 mL μm m^{-2} day^{-1} MPa^{-1} while PLACN3 (smectite clay content 4 wt %) has 120 × 10^3 mL μm m^{-2} day^{-1} MPa^{-1}. As expected, the barrier property of the nanocomposite

is higher than that of PLA, and with increasing clay content it also increases. If we compare with the clay dimensions, at the same clay loading the permeability of the mica nanocomposite (PLACN9) is higher (144×10^3 mL μm m^{-2} day^{-1} MPa^{-1}) than that of the smectite nanocomposite (PLACN3). The MMT nanocomposite has permeability similar to that of the smectite.

The barrier property depends on the particle size as well as on the dispersion. When dispersion is on the same order, it depends on the size of the particles and vice versa. Smectite being a good dispersed system, its barrier property is higher, but as the mica system has stacked layers, the barrier property is smaller, even though the size is greater. The size of the MMT nanocomposite is greater compared to the smectite one and moderately well-dispersed compared to that of the mica system; as a result, the barrier property is almost the same as the smectite one. Like mechanical property, here, again dispersion has a stronger effect than the aspect ratio, which is ultimately reflected on the final property. Gusev and Lusti[23] considered the barrier property in two ways: (1) geometric factor that favors the reduction in permeability by forcing diffusing molecules to take a long way around the platelets and (2) changes in the local permeability due to molecular level transformation in the matrix polymer in the presence of silicate layers. The first factor depends only on the size but the second factor is related to the molecular level interaction of the matrix polymer with silicate layers. The smectite system being well-dispersed, the intimate interaction between PLA and silicate layers may cause the local environment to be stiffer. As a result, both the modulus and barrier property increase compared to those of the mica system.

Porous Ceramic from Nanocomposite. The morphology of the fracture surface of porous ceramic is presented in Figure 8 obtained from (a) PLACN10, (b) PLACN7, and (c) PLACN4 after burning respective PLACNs at 950 °C. The clay content was the same in all cases (5 wt %). The white part in the figures is the edge of the stacked silicate layers. It is clear from the figures that porous ceramic material obtained from mica nanocomposite (PLACN10, Figure 8a) exhibits a distinct platelet-like morphology while smectite nanocomposite (PLACN4) shows a continuous structure. Ceramic material from MMT nanocomposite (PLACN7) is of the intermediate type. The thickness of the platelet of the materials from PLANCN10 and PLACN7 are 0.5 ± 0.2 and 0.3 ± 0.1 μm, respectively. From WAXD and TEM micrographs it is evident that stacking in MMT and mica nanocomposite is high enough and that stacking increased in porous ceramic due to the diffusion of platelets while burning. In our previous publication,[24] we report the open cell structure, morphology, and stress strain behavior of porous ceramic materials obtained from PLA nanocomposites. Now, it is necessary to find a suitable mechanism for porous ceramic material formation by burning and its clay dependency. The degradation of PLA starts at 300 °C and we kept the sample at 350 °C for 1 h, during which many of the PLA molecules degrade and the viscosity of the system gradually decreases. Then the silicate galleries can slip and take shape depending on the nature and extent of intercalation as the intercalated polymer chains degrade at a slower rate compared to the polymer molecules in bulk. The size being greater in mica, the slippage of layers is a bit difficult due to the intercalated structure and ultimately a platelet-like structure is formed. The smectite clay particle size is small enough that it thus flows easily in a well-dispersed system and finally takes a continuous type of structure. MMT being the intermediate type, layers can flow but the platelet structure remained, resulting in a continuous platelet structure. Anyway, this is the first time we are reporting the formation of porous ceramic foam obtained from various clays (clay dependency) from polymer/layered silicate nanocomposites and its mechanism of formation.

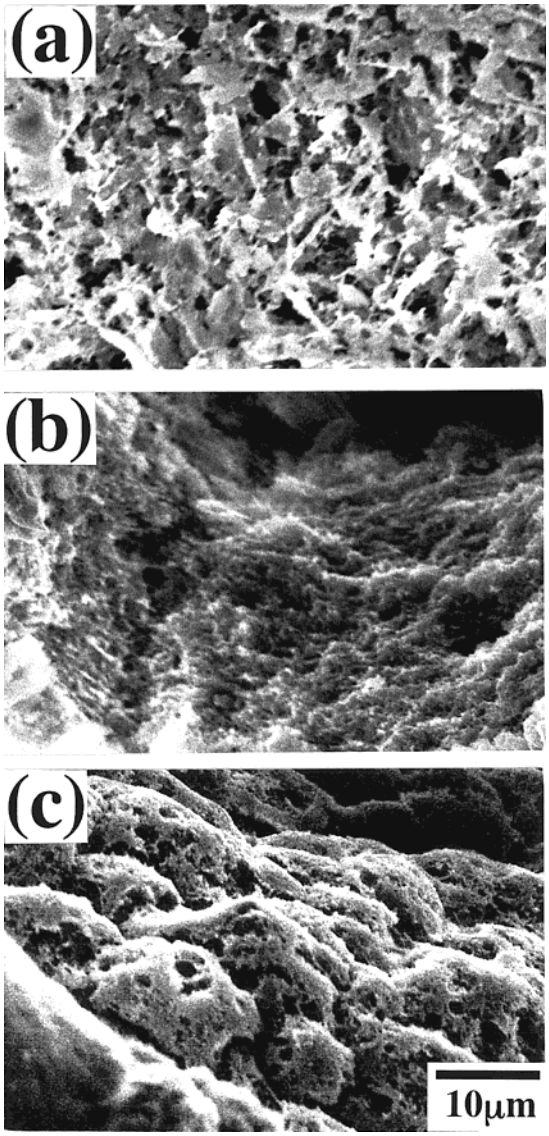

Figure 8. Scanning electron micrographs of porous ceramic materials obtained after burning the nanocomposites with C_{16} modifier and same clay content (5 wt %): (a) PLACN10 (mica), (b) PLACN7 (MMT), and (c) PLACN4 (smectite).

Conclusion

Miscibility of an organic modifier (phosphonium salt) and PLA is enhanced with a higher chain length of modifier. For a particular type of clay silicate, gallery

(23) Gusev, A. A.; Lusti, H. R. *Adv. Mater.* **2001**, *13*, 1641.
(24) SinhaRay, S.; Okamoto, K.; Yamada, K.; Okamoto, M. *Nano Lett.* **2002**, *2*, 423.

spacing ($d_{(001)}$) increases with increasing chain length of organic modifier, and for a certain organic modifier, $d_{(001)}$ increases with clay dimension due to the higher CEC and restricted conformation of modifier inside the core of the layers due to physical jamming. The increment of modulus of smectite nanocomposites compared to that of PLA is high because of its better dispersion of clay particles while this increment is smaller in the case of mica nanocomposites, even though it has a higher aspect ratio, as most of the silicate layers remain stacked. The gas barrier property of the smectite nanocomposite is higher than the mica type as the dispersion is better in the smectite type and hence the extent of interaction between PLA and silicate layers is enhanced and those effects overcome the dimensional effect of the mica system. Porous ceramic material obtained by burning of PLA nanocomposites and its variation in different clay particle sizes is reported for the first time with the mechanism of its formation.

Acknowledgment. This work was partially supported by the Grant-in-Aid for Academic Frontier Center under the project "Future Data Storage Materials" granted by the Ministry of Education, Science, Sports and Culture, Japan (1999−2003).

CM020391B